The Astrophysical Journal, 644:971–980, 2006 June 20

RANDOM WALK OF MAGNETIC FIELD LINES IN NONAXISYMMETRIC TURBULENCE

D. Ruffolo,[1] P. Chuychai,[1,2,3] and W. H. Matthaeus[3]
Received 2005 December 23; accepted 2006 February 22

ABSTRACT

The random walk of turbulent magnetic field lines strongly affects transport of energetic particles in astrophysical plasmas, but is not well understood for general configurations that lack rotational symmetry. Here we derive nonperturbative field-line diffusion coefficients for magnetic fluctuations that are nonaxisymmetric with respect to the mean magnetic field. We consider a superposition of slab plus two-dimensional fluctuations, a model that has proven useful in heliospheric studies. Two independent parameters are introduced to allow polarization of the slab component and stretching of the two-dimensional component. With the assumptions of homogeneity, the diffusion approximation, and Corrsin's independence hypothesis, we derive two coupled biquadratic equations for the diffusion coefficients. The results and underlying assumptions are confirmed by numerical simulations. Special cases of interest include the counterintuitive results that enhanced fluctuations in one direction lead to decreased diffusion in the other direction, and that extreme nonaxisymmetry leads to diffusion coefficients proportional to the rms two-dimensional fluctuation.

Subject headings: diffusion — magnetic fields — turbulence

1. INTRODUCTION

Turbulent motions, nearly universal in tenuous astrophysical plasmas, lead to magnetic turbulence and the random walk of magnetic field lines. The field lines define the magnetic topology and play an important physical role by guiding the motion of charged particles. The classic work of Jokipii (1966) and Jokipii & Parker (1968) expressed a relationship between the random walk of field lines in magnetic turbulence and the diffusion of energetic charged particles perpendicular to the mean magnetic field in astrophysical plasmas, for the case of weak fluctuations, often described as the quasi-linear (QLT) limit.

Recent work on the field-line random walk has stressed the importance of large amplitude fluctuations, as well as the generally anisotropic character of magnetohydrodynamic (MHD) turbulence (Isichenko 1991a, 1991b; Wang et al. 1995; Matthaeus et al. 1995; Pommois et al. 1999). This involves not only extending the analytical methods beyond the QLT approach, but also appropriately representing more complex three-dimensional magnetic turbulence properties. In particular, a two-component "2D+slab" model adds slab and two-dimensional turbulence to provide a useful model of solar wind fluctuations (Matthaeus et al. 1990; Bieber et al. 1996). This model of anisotropic turbulence is sufficiently simple to allow analytic calculations of ensemble average properties while still including a rich variety of local topological effects (Ruffolo et al. 2003; Chuychai et al. 2005). The anisotropy is strong in the low-latitude solar wind, with a roughly 80 : 20 ratio of two-dimensional to slab turbulent energy (Bieber et al. 1994, 1996), and is even stronger in magnetic clouds (Leamon et al. 1998) and rarefaction regions in the solar wind (Smith et al. 2001, 2004). Recent results suggest that the fast wind has a lower two-dimensional admixture, with perhaps a 50 : 50 ratio of energies (Dasso et al. 2005). The anisotropic nature of solar wind turbulence has been shown to have interesting physical effects. Bieber et al. (1994) showed that this anisotropy may resolve the long-standing discrepancy between theoretical and observed mean free paths of solar energetic particles. Matthaeus et al. (1995) derived analytic formulae for the field-line random walk in two-component turbulence—later confirmed by computer simulations (Gray et al. 1996)—that indicates diffusion tending as b^2/B_0^2 for slab turbulence (Jokipii & Parker 1968) but as b/B_0 for the two-dimensional component. Note, however, that many of the classic concepts of transport phenomena in turbulent media are based on implicit assumptions of nearly isotropic turbulence. Ruffolo et al. (2004) showed that in two-component turbulence, the separation of magnetic field lines only develops an exponential form (Rechester & Rosenbluth 1978) when the slab component dominates the field-line random walk, and the Kubo number that classically defines quasi-linear versus percolative behavior (e.g., Isichenko 1991a, 1991b) needs to be modified for strongly anisotropic turbulence.

Understanding has greatly improved by considering the anisotropy of magnetic turbulence; however, most of this work has continued to assume *axisymmetry*, with some notable exceptions (e.g., Pommois et al. 1999, 2001). Axisymmetry about the z-axis (usually the coordinate along the mean field) implies that statistical properties of the turbulent field are rotationally symmetric in the perpendicular coordinates x and y. However, there are indications that the variances of magnetic fluctuations may be nonaxisymmetric in some cases of interest. The classic work of Belcher & Davis (1971) indicated a roughly 4 : 3 ratio in solar wind fluctuation energy in the $\hat{z} \times \hat{r}$ direction relative to the orthogonal direction (see Table 6 of Belcher & Davis 1971) along the *Mariner 5* Venus flyby trajectory. Recent studies also suggest a possible role of nonaxisymmetric fluctuations in enhanced latitudinal transport of cosmic rays at high heliographic latitudes (Jokipii et al. 1995; Burger & Hattingh 1998). Note that the Archimedean spiral magnetic field (Parker 1958) in the outer heliosphere is mainly in the azimuthal direction, so the two perpendicular coordinates are r and θ. However, the mean solar wind flow is essentially radial with a small deceleration, so the solar wind plasma is greatly stretched in θ with a slight compression in r. Furthermore, there are various intermittent structures that can interrupt coherence in the r-direction, such as corotating interaction regions, coronal mass ejections, shocks, and the

[1] Department of Physics, Faculty of Science, Mahidol University, Bangkok 10400, Thailand; david_ruffolo@yahoo.com.
[2] Department of Physics, Faculty of Science, Chulalongkorn University, Bangkok 10330, Thailand; paeng@bartol.udel.edu.
[3] Bartol Research Institute, University of Delaware, Newark, DE 19716; yswhm@bartol.udel.edu.

heliospheric current sheet. Because these effects can lead to both different energies and different correlation scales in the two components of turbulence (two-dimensional and slab) and in the two directions perpendicular to the mean magnetic field, one might expect substantial nonaxisymmetry of magnetic turbulence in the outer heliosphere (Jokipii 1973), even if there is some transfer of energy between the two perpendicular directions due to dynamical couplings. For these reasons there is ample motivation to extend our understanding of axisymmetric turbulence to the more general case of nonaxisymmetry.

In this work we develop a theory for the nonaxisymmetric field-line random walk in a general nonperturbative scheme (Matthaeus et al. 1995). This approach is useful for transverse fluctuations in general, and is explicitly applied here to nonaxisymmetric two-component turbulence. The nonaxisymmetry includes both polarization of the slab component and stretching of the two-dimensional component in wavenumber space. Our principal result is a set of coupled biquadratic equations in the diffusion coefficients D_x and D_y. Computer simulations are also performed, which verify the analytic solutions and justify the underlying assumptions. An interesting finding is that increased fluctuations in one direction can inhibit the field-line random walk in the other direction. It is also found that the limit of extreme nonaxisymmetry leads to a first-order dependence of the field-line random walk on b/B_0. We derive closed-form solutions for several limiting cases, which should find immediate application in heliospheric scattering problems such as cosmic-ray modulation.

2. ANALYTIC THEORY

The present work considers statistically homogeneous, nonaxisymmetric two-component magnetic turbulence. In the two-component model, we assume

$$\boldsymbol{B} = \boldsymbol{B}_0 + \boldsymbol{b}(x, y, z), \tag{1}$$

where the mean field $\boldsymbol{B}_0$ is constant. We also use

$$\boldsymbol{B}_0 = B_0 \hat{z}, \quad \boldsymbol{b} \perp \hat{z}, \tag{2}$$

and the fluctuating field, of mean zero, is given by

$$\boldsymbol{b} = \boldsymbol{b}^{\rm 2D}(x, y) + \boldsymbol{b}^{\rm slab}(z). \tag{3}$$

For brevity, we refer to a quantity such as $\langle b^2 \rangle$ as the magnetic energy of the fluctuations, E, and define $b \equiv \langle b^2 \rangle^{1/2}$. In general, we can write

$$\boldsymbol{b}^{\rm 2D}(x, y) = \nabla \times [a(x, y)\hat{z}]. \tag{4}$$

The potential function $a(x, y)$ can be taken to be a random function fluctuating about a constant mean value, taken to be zero for convenience, with a well-behaved power spectrum $A(k_x, k_y)$ (Ruffolo et al. 2004).

In the absence of a slab component, the field lines for two-dimensional turbulence would move along curves of constant a, since equation (4) indicates that $\boldsymbol{b}^{\rm 2D} \perp \nabla a$. In three dimensions, such field lines are constrained to flux tubes that are "cylinders" in the mathematical sense of surfaces of constant $a(x, y)$. This can account for the repeated dropouts in observations of solar energetic particles from impulsive solar flares (Mazur et al. 2000; Ruffolo et al. 2003). A key feature that makes the two-component model of turbulence realistic and interesting is that the slab component imposes random perturbations on the field-line motion, leading to mixing of field lines and wandering to regions of different $a(x, y)$ (see also Matthaeus et al. 1995).

Note that $B_z \equiv B_0$, so in this model it is impossible for a magnetic field line to backtrack in the z-direction, and the z-coordinate specifies a unique location along a magnetic field line. Therefore, we follow the standard practice of defining the field-line diffusion coefficient in terms of the distance Δz:

$$D_x = \frac{\left\langle (\Delta x)^2 \right\rangle}{2\Delta z}$$
$$D_y = \frac{\left\langle (\Delta y)^2 \right\rangle}{2\Delta z}. \tag{5}$$

For nonaxisymmetric turbulence, we note that $\langle (\Delta x)^2 \rangle \neq \langle (\Delta y)^2 \rangle$. To obtain a nonaxisymmetric slab field, we can explicitly set the parallel correlation length, l_c, and rms slab magnitude, $b^{\rm slab} \equiv (\langle b^2 \rangle^{\rm slab})^{1/2}$, to be different in the x- and y-directions. For two-dimensional turbulence, the power spectrum $A(k_x, k_y)$ for the axisymmetric case depends only on $k_\perp = (k_x^2 + k_y^2)^{1/2}$; i.e., it is constant along circles in (k_x, k_y) space. To consider nonaxisymmetric two-dimensional turbulence, we use a form that is instead constant along ellipses in (k_x, k_y) space (Fig. 1). Note that our model incorporates the two key ways to violate axisymmetry: (1) a difference between the two "polarizations" (for the slab component), and (2) a difference between correlation scales in different directions (for the two-dimensional component).

Our analytic derivation of D_x and D_y follows those of Matthaeus et al. (1995) and Ruffolo et al. (2004) in assuming Corrsin's independence hypothesis (Corrsin 1959; Salu & Montgomery 1977; see also McComb 1990), Gaussian random walk distributions, and diffusive behavior. Computer simulations have been used to verify the validity of these assumptions for the field-line random walk (Gray et al. 1996) and field-line separation (Ruffolo et al. 2004) in two-component turbulence.

Following Jokipii & Parker (1969), we express the change in the x- and y-coordinates of a field line over a distance Δz along the mean magnetic field as

$$\Delta x \equiv x(\Delta z) - x(0) = \frac{1}{B_0}\int_0^{\Delta z} b_x[x(z'), y(z'), z']\, dz'$$
$$\Delta y \equiv y(\Delta z) - y(0) = \frac{1}{B_0}\int_0^{\Delta z} b_y[x(z'), y(z'), z']\, dz'. \tag{6}$$

The ensemble average of $(\Delta x)^2$ is then given by

$$\left\langle \Delta x^2 \right\rangle = \frac{1}{B_0^2}\int_0^{\Delta z}\int_0^{\Delta z} \langle b_x[x(z'), y(z'), z'] b_x[x(z''), y(z''), z'']\rangle dz' dz''$$
$$= \frac{1}{B_0^2}\int_0^{\Delta z}\int_0^{\Delta z} \langle b_x(x', y', z') b_x(x'', y'', z'')\rangle\, dz'\, dz'', \tag{7}$$

where we introduce the notation x' for $x(z')$, etc. We can also write

$$\left\langle \Delta x^2 \right\rangle = \frac{1}{B_0^2}\int_0^{\Delta z}\int_{-z'}^{\Delta z - z'} \langle b_x(x', y', z') b_x(x'', y'', z' + \Delta z')\rangle\, d\Delta z' dz', \tag{8}$$

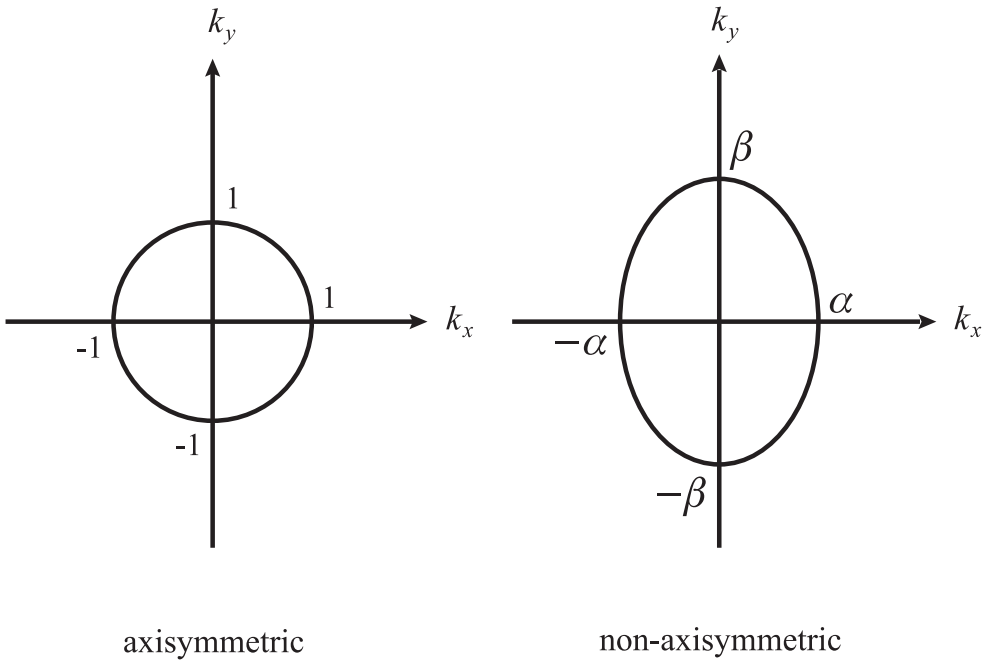

FIG. 1.—Contours of constant power $A(k_x, k_y)$ of the two-dimensional potential function for the axisymmetric model and for our nonaxisymmetric model. To maintain the same turbulent energy, we can set $\alpha = 1/\xi^{1/2}$ and $\beta = \xi^{1/2}$, where ξ is an ellipticity parameter.

where $\Delta z' \equiv z'' - z'$, and with the assumption of homogeneity,

$$\langle \Delta x^2 \rangle = \frac{1}{B_0^2} \int_0^{\Delta z} \int_{-z'}^{\Delta z - z'} \langle b_x(0, 0, 0) b_x(\Delta x', \Delta y', \Delta z') \rangle \, d\Delta z' \, dz', \tag{9}$$

where $\Delta x' \equiv x'' - x'$ and $\Delta y' \equiv y'' - y'$. By changing b_x to b_y we can obtain a similar formula for $\langle \Delta y^2 \rangle$.

Here we use Corrsin's hypothesis in position space and consider the Lagrangian correlation function $\langle b_x(x', y', z') b_x(x'', y'', z'') \rangle$ to be the Eulerian correlation function, $R_{xx} \equiv \langle b_x(0, 0, 0) b_x(x, y, z) \rangle$, weighted by the conditional probability of finding $(\Delta x', \Delta y')$ after a given $\Delta z'$:

$$\langle \Delta x^2 \rangle = \frac{1}{B_0^2} \int_0^{\Delta z} \int_{-z'}^{\Delta z - z'} \int_{-\infty}^{\infty} \int_{-\infty}^{\infty} R_{xx}(\Delta x', \Delta y', \Delta z') \times P(\Delta x' | \Delta z') P(\Delta y' | \Delta z') \, d\Delta x' \, d\Delta y' \, d\Delta z' \, dz'. \tag{10}$$

The formula for $\langle \Delta y^2 \rangle$ is similar:

$$\langle \Delta y^2 \rangle = \frac{1}{B_0^2} \int_0^{\Delta z} \int_{-z'}^{\Delta z - z'} \int_{-\infty}^{\infty} \int_{-\infty}^{\infty} R_{yy}(\Delta x', \Delta y', \Delta z') \times P(\Delta x' | \Delta z') P(\Delta y' | \Delta z') \, d\Delta x' \, d\Delta y' \, d\Delta z' \, dz'. \tag{11}$$

We assume the probabilities in equations (10) and (11) to be Gaussian distributions as

$$P(\Delta x' | \Delta z') = \frac{1}{\sqrt{2\pi\sigma_x^2}} \exp\left[-\frac{(\Delta x')^2}{2\sigma_x^2} \right]$$
$$P(\Delta y' | \Delta z') = \frac{1}{\sqrt{2\pi\sigma_y^2}} \exp\left[-\frac{(\Delta y')^2}{2\sigma_y^2} \right], \tag{12}$$

where σ_x^2 and σ_y^2 are the variances in x- and y-components. We apply the diffusion approximation for the variances, which are

$$\sigma_x^2 = \left\langle (\Delta x')^2 \right\rangle = 2D_x |\Delta z'|$$
$$\sigma_y^2 = \left\langle (\Delta y')^2 \right\rangle = 2D_y |\Delta z'|. \tag{13}$$

Thus, equations (12) become

$$P(\Delta x' | \Delta z') = \frac{1}{\sqrt{4\pi D_x |\Delta z'|}} \exp\left[-\frac{(\Delta x')^2}{4D_x |\Delta z'|} \right]$$
$$P(\Delta y' | \Delta z') = \frac{1}{\sqrt{4\pi D_y |\Delta z'|}} \exp\left[-\frac{(\Delta y')^2}{4D_y |\Delta z'|} \right]. \tag{14}$$

Next we integrate equations (10) and (11) over $\Delta z'$ and z' and introduce the power spectra P_{xx} and P_{yy} as the Fourier transforms of the correlation functions R_{xx} and R_{yy}, respectively. Again using the diffusion approximation, we set $\langle \Delta x^2 \rangle = 2D_x \Delta z$ and $\langle \Delta y^2 \rangle = 2D_y \Delta z$. Finally, we obtain the coupled equations for D_x and D_y as

$$D_x = \frac{\langle \Delta x^2 \rangle}{2\Delta z} = \frac{1}{\sqrt{2\pi}} \frac{1}{B_0^2} \int_{-\infty}^{\infty} \frac{1 - \cos(k_z \Delta z)}{k_z^2 \Delta z} P_{xx}^{\text{slab}}(k_z) \, dk_z + \frac{1}{2\pi} \frac{1}{B_0^2} \int_{-\infty}^{\infty} \int_{-\infty}^{\infty} \frac{P_{xx}^{\text{2D}}(k_x, k_y)}{(D_x k_x^2 + D_y k_y^2)} \times \left\{ 1 - g\left[\left(D_x k_x^2 + D_y k_y^2 \right) \Delta z \right] \right\} dk_x \, dk_y,$$
$$D_y = \frac{\langle \Delta y^2 \rangle}{2\Delta z} = \frac{1}{\sqrt{2\pi}} \frac{1}{B_0^2} \int_{-\infty}^{\infty} \frac{1 - \cos(k_z \Delta z)}{k_z^2 \Delta z} P_{yy}^{\text{slab}}(k_z) \, dk_z + \frac{1}{2\pi} \frac{1}{B_0^2} \int_{-\infty}^{\infty} \int_{-\infty}^{\infty} \frac{P_{yy}^{\text{2D}}(k_x, k_y)}{\left(D_x k_x^2 + D_y k_y^2 \right)} \times \left\{ 1 - g\left[\left(D_x k_x^2 + D_y k_y^2 \right) \Delta z \right] \right\} dk_x \, dk_y, \tag{15}$$

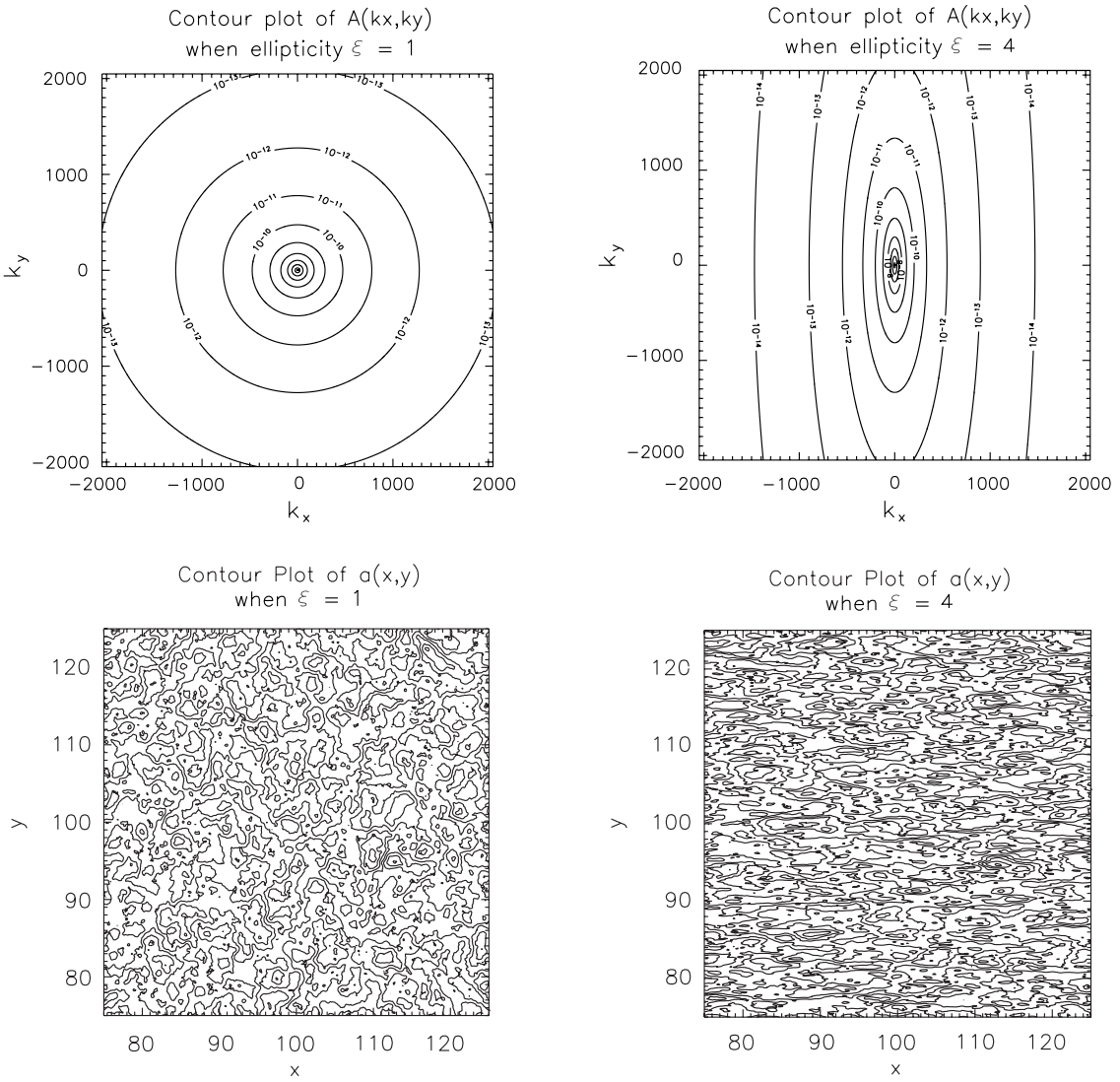

FIG. 2.—Contours of constant power $A(k_x, k_y)$ for axisymmetric ($\xi = 1$, *top left*) and nonaxisymmetric ($\xi = 4$, *top right*) cases, and contours of corresponding representations of the potential function $a(x, y)$ ($\xi = 1$, *bottom left*; $\xi = 4$, *bottom right*). Note that the two-dimensional component of magnetic turbulence, $\boldsymbol{b}^{2D}(x, y) = \nabla \times [a(x, y)\hat{z}]$, follows the contours of constant $a(x, y)$.

where $g(u) \equiv (1 - e^{-u})/u$ behaves as a low-pass filter; i.e., $g(u) \approx 1$ for $u \ll 1$ and monotonically declines to zero as $u \rightarrow \infty$.

Following Ruffolo et al. (2004), when we choose a large Δz, equations (15) become

$$D_x - D_x^{\rm slab} = \frac{1}{2\pi}\frac{1}{B_0^2}\int_{-\infty}^{\infty}\int_{-\infty}^{\infty}\frac{P_{xx}^{2D}(k_x,k_y)}{(D_x k_x^2 + D_y k_y^2)}\,dk_x\,dk_y$$

$$D_y - D_y^{\rm slab} = \frac{1}{2\pi}\frac{1}{B_0^2}\int_{-\infty}^{\infty}\int_{-\infty}^{\infty}\frac{P_{yy}^{2D}(k_x,k_y)}{(D_x k_x^2 + D_y k_y^2)}\,dk_x\,dk_y, \quad (16)$$

where

$$D_x^{\rm slab} = \sqrt{\frac{\pi}{2}}\,\frac{P_{xx}^{\rm slab}(0)}{B_0^2} = \frac{l_x f_{sx} b^2}{B_0^2} \quad (17)$$

$$D_y^{\rm slab} = \sqrt{\frac{\pi}{2}}\,\frac{P_{yy}^{\rm slab}(0)}{B_0^2} = \frac{l_y f_{sy} b^2}{B_0^2}. \quad (18)$$

Here l_x and l_y are the correlation lengths in the x- and y-directions, respectively, f_{sx} is the fraction of turbulent energy that is slab energy in the x-direction, $f_{sx} = \langle b_x^2 \rangle^{\rm slab}/\langle b^2 \rangle$, and similarly f_{sy} is the fraction that is slab energy in the y-direction.

Equations (17) and (18), which correspond to the results of Jokipii & Parker (1968), make it clear how nonaxisymmetry affects the field-line random walk due to the slab component of turbulence. The effect on the two-dimensional component is not as clear, especially because $P_{xx}^{2D}(k_x, k_y)$ and $P_{yy}^{2D}(k_x, k_y)$ are not independent functions. From equation (4), which relates $\boldsymbol{b}^{2D}(x, y)$ to the potential function $a(x, y)$, we infer that $P_{xx}^{2D} = k_y^2 A$ and $P_{yy}^{2D} = k_x^2 A$, where $A(k_x, k_y)$ is the power spectrum of $a(x, y)$. Thus, nonaxisymmetry in the two-dimensional component of the turbulent magnetic field is generated by nonaxisymmetry in $A(k_x, k_y)$.

For the axisymmetric case, $A(k_x, k_y)$ is constant along circles of constant $k_\perp = (k_x^2 + k_y^2)^{1/2}$ in (k_x, k_y) space, so $A = A(k_\perp)$. For the nonaxisymmetric case, we model the two-dimensional component by taking $A(k_x, k_y)$ to be constant along ellipses in (k_x, k_y) space that have a major to minor axis ratio of β/α (see Fig. 1). We refer to this ratio as the ellipticity parameter ξ, and Figure 2 shows examples of $A(x, y)$ and representations of the two-dimensional potential function $a(x, y)$ for $\xi = 1$

(axisymmetric case) and $\xi = 4$ (a nonaxisymmetric case). Note that using $\xi \neq 1$ stretches the "islands" of constant $a(x, y)$. Now we write $k'_x = k_x/\alpha$, $k'_y = k_y/\beta$, and $k'_\perp = (k'^2_x + k'^2_y)^{1/2} = (k_x^2/\alpha^2 + k_y^2/\beta^2)^{1/2}$ and assume $A = A(k'_\perp)$. This yields

$$D_x - D_x^{\rm slab} = \frac{1}{2\pi}\frac{1}{B_0^2}\int_{-\infty}^{\infty}\int_{-\infty}^{\infty}\frac{\beta^2 k'^2_y A(k'_\perp)}{\left(D_x\alpha^2 k'^2_x + D_y\beta^2 k'^2_y\right)} d(\alpha k'_x) d(\beta k'_y)$$

$$D_y - D_y^{\rm slab} = \frac{1}{2\pi}\frac{1}{B_0^2}\int_{-\infty}^{\infty}\int_{-\infty}^{\infty}\frac{\alpha^2 k'^2_x A(k'_\perp)}{\left(D_x\alpha^2 k'^2_x + D_y\beta^2 k'^2_y\right)} d(\alpha k'_x)\, d(\beta k'_y). \quad (19)$$

Next, we write equations (19) in polar coordinates $k'_\perp$ and θ such that $k'_x = k'_\perp \cos\theta$ and $k'_y = k'_\perp \sin\theta$:

$$D_x - D_x^{\rm slab} = \frac{\alpha\beta}{2\pi B_0^2}\int_0^{2\pi}\int_0^{\infty}\frac{\beta^2 k'^2_\perp \sin^2\theta A(k'_\perp)}{\left(D_x\alpha^2 k'^2_\perp\cos^2\theta + D_y\beta^2 k'^2_\perp \sin^2\theta\right)} k'_\perp dk'_\perp d\theta$$
$$= \frac{\alpha\beta}{2\pi B_0^2 D_x}\frac{\beta^2}{\alpha^2}\int_0^{\infty} A(k'_\perp) k'_\perp dk'_\perp \times \int_0^{2\pi}\frac{1}{\cot^2\theta + (\beta^2/\alpha^2)(D_y/D_x)}\, d\theta$$

$$D_y - D_y^{\rm slab} = \frac{\alpha\beta}{2\pi B_0^2}\int_0^{2\pi}\int_0^{\infty}\frac{\alpha^2 k'^2_\perp \cos^2\theta A(k'_\perp)}{\left(D_x\alpha^2 k'^2_\perp\cos^2\theta + D_y\beta^2 k'^2_\perp \sin^2\theta\right)} k'_\perp dk'_\perp d\theta$$
$$= \frac{\alpha\beta}{2\pi B_0^2 D_x}\int_0^{\infty} A(k'_\perp) k'_\perp dk'_\perp \times \int_0^{2\pi}\frac{1}{1 + (\beta^2/\alpha^2)(D_y/D_x)\tan^2\theta}\, d\theta. \quad (20)$$

Note that

$$\int_0^{\infty}\left[1/\left(\cot^2\theta + \rho^2\right)\right] d\theta = \frac{2\pi}{[\rho(\rho+1)]} \quad (21)$$

and

$$\int_0^{\infty}\left[1/\left(1 + \rho^2\tan^2\theta\right)\right] d\theta = \frac{2\pi}{(\rho+1)}, \quad (22)$$

where $\rho = (\beta/\alpha)(D_y/D_x)^{1/2}$ in our integrals. Then we obtain

$$D_x - D_x^{\rm slab} = \left[\frac{\alpha\beta}{B_0^2}\int_0^{\infty} A(k'_\perp) k'_\perp dk'_\perp\right] \times \frac{\beta^2}{\alpha^2 D_x}\frac{1}{(\beta/\alpha)\sqrt{D_y/D_x}\left[1 + (\beta/\alpha)\sqrt{D_y/D_x}\right]}$$

$$D_y - D_y^{\rm slab} = \left[\frac{\alpha\beta}{B_0^2}\int_0^{\infty} A(k'_\perp) k'_\perp dk'_\perp\right] \times \frac{1}{D_x}\frac{1}{\left[1 + (\beta/\alpha)\sqrt{D_y/D_x}\right]}. \quad (23)$$

Let us define I to be the term in parentheses:

$$I = \frac{\alpha\beta}{B_0^2}\int_0^{\infty} A(k'_\perp) k'_\perp dk'_\perp. \quad (24)$$

Transforming $k'_\perp$ back to k_x and k_y,

$$I = \frac{1}{2\pi B_0^2}\int_{-\infty}^{\infty}\int_{-\infty}^{\infty} A(k_x, k_y) dk_x\, dk_y = \frac{\langle a^2\rangle}{B_0^2} = \left(\tilde{\lambda}\frac{b^{\rm 2D}}{B_0}\right)^2 = 2\left(D_\perp^{\rm 2D}\right)^2, \quad (25)$$

where $\tilde{\lambda}$ is called the "ultrascale" (Matthaeus et al. 1995). Combining equations (23) and (24), we obtain the coupled biquadratic equations for the field-line random walk in a nonaxisymmetric two-component model of magnetic turbulence:

$$\left(D_x - D_x^{\rm slab}\right)\left(D_y + \frac{\alpha}{\beta}\sqrt{D_x D_y}\right) = I$$
$$\left(D_y - D_y^{\rm slab}\right)\left(D_x + \frac{\beta}{\alpha}\sqrt{D_x D_y}\right) = I. \quad (26)$$

In terms of the ellipticity parameter $\xi = \beta/\alpha$ we have

$$\left(D_x - D_x^{\rm slab}\right)\left(D_y + \frac{\sqrt{D_x D_y}}{\xi}\right) = I$$
$$\left(D_y - D_y^{\rm slab}\right)\left(D_x + \xi\sqrt{D_x D_y}\right) = I. \quad (27)$$

These equations are straightforward to solve numerically for a given case of interest, and in § 3 we derive closed-form solutions for certain limiting cases.

3. INTERPRETATION

To solve the coupled biquadratic equations (27), a "user" of the calculation needs to specify certain physical inputs:

B_0—the mean magnetic field.
b—the rms turbulent magnetic field.
f_s—the slab fraction of turbulent energy.
$\eta^2 \equiv f_{sx}/f_{sy}$—the slab anisotropy.
l_x—the correlation length of $b_x^{\rm slab}$.
l_y—the correlation length of $b_y^{\rm slab}$.
$\tilde{\lambda}$—the ultrascale (of two-dimensional turbulence).
ξ—the ellipticity parameter.

Actually, instead of providing both b and B_0, it is sufficient to specify only their ratio. The two anisotropy parameters η and ξ are quite distinct physically; we show shortly that ξ is also the anisotropy of the field-line diffusion coefficients for the two-dimensional component alone: $\xi^2 = D_x^{\rm 2D}/D_y^{\rm 2D}$. In terms of these inputs, the quantities in equations (27) are given as

$$D_x^{\rm slab} = \frac{\eta^2}{\eta^2+1}\frac{l_x f_s b^2}{B_0^2} \quad (28)$$

$$D_y^{\rm slab} = \frac{1}{\eta^2+1}\frac{l_y f_s b^2}{B_0^2}. \quad (29)$$

$$I = (1 - f_s)\left(\tilde{\lambda}\frac{b}{B_0}\right)^2, \quad (30)$$

and from equation (25) we have $I = 2(D_\perp^{\rm 2D})^2$, so

$$D_\perp^{\rm 2D} = \sqrt{\frac{1-f_s}{2}}\tilde{\lambda}\frac{b}{B_0}. \quad (31)$$

Note that $D_x^{\rm slab}$ and $D_y^{\rm slab}$ depend on $(b/B_0)^2$, whereas $D_\perp^{\rm 2D} \propto b/B_0$ (see also Taylor & McNamara 1971).

Let us stress that the results in § 2 apply for general and independent functional forms of $P_{xx}^{\rm slab}(k_z)$, $P_{yy}^{\rm slab}(k_z)$, and $A(k'_\perp)$. For the slab fluctuations, we allow a general polarization in the sense that x- and y-polarizations have independent power spectra, and we see that the calculation depends only on the product $l_i f_{si}$, where $i = x$ or y. For the two-dimensional fluctuations, we take $A(k_x, k_y)$ to be stretched in one direction relative to the axisymmetric configuration (Figs. 1 and 2). Thus, the slab anisotropy η and ellipticity ξ represent physically distinct types of nonaxisymmetry.

In many applications, direct measurements of the physical inputs are not available, so one must make educated guesses or *ad hoc* approximations. Here we present solutions of the general equations (27) for specific limits and approximations. Naturally, the simplest approximation is that either slab or two-dimensional turbulence can be neglected. For the case where two-dimensional turbulence is absent, we have $f_s = 1$, $I = 0$, $D_x = D_x^{\rm slab}$, and $D_y = D_y^{\rm slab}$, so we recover the Jokipii & Parker (1968) results for slab turbulence as in equations (28) and (29).

Next, consider the limit at which the slab fraction goes to zero. It is useful to define the geometric mean of overall diffusion coefficients, $D_\perp \equiv (D_x D_y)^{1/2}$, and an anisotropy of overall diffusion coefficients, $\delta \equiv (D_x/D_y)^{1/2}$. Setting $D_x^{\rm slab} = D_y^{\rm slab} = 0$, equations (27) give

$$D_\perp^2\left(1+\frac{\delta}{\xi}\right) = I$$
$$D_\perp^2\left(1+\frac{\xi}{\delta}\right) = I, \tag{32}$$

which are only satisfied for $\delta = \xi$, giving $D_\perp = (I/2)^{1/2} = D_\perp^{\rm 2D}$ as in Matthaeus et al. (1995). Therefore,

$$D_x = \delta D_\perp = \xi D_\perp^{\rm 2D}$$
$$D_y = \frac{D_\perp}{\delta} = \frac{D_\perp^{\rm 2D}}{\xi}, \tag{33}$$

and we can indeed interpret ξ as the anisotropy of the field-line random walk for two-dimensional turbulence, $\xi = (D_x^{\rm 2D}/D_y^{\rm 2D})^{1/2}$.

Now suppose that both the slab and two-dimensional components are present. If η and ξ are not known, a simple approximation is to set them equal ($\eta = \xi$). Let us also set $l_x = l_y = l$, which along with equations (28) and (29) implies that $\eta = (D_x^{\rm slab}/D_y^{\rm slab})^{1/2}$. Then from an argument similar to that for the pure two-dimensional case, it can be shown that $\delta = \xi$ as well. Therefore, equations (27) decouple to these two equations:

$$\left(D_x - D_x^{\rm slab}\right)\left(\frac{D_x}{\xi^2}\right) = \frac{I}{2}$$
$$\left(D_y - D_y^{\rm slab}\right)\left(\xi^2 D_y\right) = \frac{I}{2}. \tag{34}$$

The solutions for this case are

$$D_x = \frac{1}{2}\left[D_x^{\rm slab} + \sqrt{(D_x^{\rm slab})^2 + 4\left(D_x^{\rm 2D}\right)^2}\right]$$
$$D_y = \frac{1}{2}\left[D_y^{\rm slab} + \sqrt{(D_y^{\rm slab})^2 + 4\left(D_y^{\rm 2D}\right)^2}\right], \tag{35}$$

which is the same as the formula obtained by Matthaeus et al. (1995) but now applied separately to D_x and D_y quantities. In terms of the physical inputs, we have

$$D_x = \frac{1}{2}\left[\frac{\xi^2}{\xi^2+1}\frac{lf_s b^2}{B_0^2} + \sqrt{\left(\frac{\xi^2}{\xi^2+1}\frac{lf_s b^2}{B_0^2}\right)^2 + 4\xi^2 (D_\perp^{\rm 2D})^2}\right]$$
$$D_y = \frac{1}{2}\left[\frac{1}{\xi^2+1}\frac{lf_s b^2}{B_0^2} + \sqrt{\left(\frac{1}{\xi^2+1}\frac{lf_s b^2}{B_0^2}\right)^2 + 4\frac{\left(D_\perp^{\rm 2D}\right)^2}{\xi^2}}\right]. \tag{36}$$

Now, further suppose that the turbulence is extremely nonaxisymmetric, i.e., that all other input values are fixed but η and ξ both tend to 0 or both tend to ∞. Then, from equations (36) it can be seen that the two-dimensional contribution dominates. That is, when ξ tends to zero, $D_x \to \xi D_\perp^{\rm 2D}$ and $D_y \to D_\perp^{\rm 2D}/\xi$. Similarly, as ξ goes to ∞, we again have $D_x \to \xi D_\perp^{\rm 2D}$ and $D_y \to D_\perp^{\rm 2D}/\xi$. Such extreme nonaxisymmetry might occur in the outer heliosphere if field fluctuations are "frozen in" the solar wind as it expands very differently in the two perpendicular directions.

Now let us return to the general case of any possible input parameters. For convenience in analyzing the coupled equations (27), we can rewrite all variables to compare with the two-dimensional values, yielding

$$D'_\perp = \frac{D_\perp}{D_\perp^{\rm 2D}}, \qquad D_\perp^{s\prime} = \frac{D_\perp^{\rm slab}}{D_\perp^{\rm 2D}}, \tag{37}$$

$$\delta' = \frac{\delta}{\xi} = \frac{\sqrt{D_x/D_y}}{\sqrt{D_x^{\rm 2D}/D_y^{\rm 2D}}}, \tag{38}$$

$$\eta' = \frac{\eta\sqrt{l_x/l_y}}{\xi} = \frac{\sqrt{D_x^{\rm slab}/D_y^{\rm slab}}}{\sqrt{D_x^{\rm 2D}/D_y^{\rm 2D}}}, \tag{39}$$

where we define $D_\perp$, $D_\perp^{\rm 2D}$, and $D_\perp^{\rm slab}$ as the geometric means $(D_x D_y)^{1/2}$, $(D_x^{\rm 2D} D_y^{\rm 2D})^{1/2}$, and $(D_x^{\rm slab} D_y^{\rm slab})^{1/2}$, respectively. Now equations (27) become two coupled equations with two unknown parameters, $D'_\perp$ and δ':

$$D'_\perp\left(\frac{1}{\delta'}+1\right)\left(\delta' D'_\perp - \eta' D_\perp^{s\prime}\right) = 2$$
$$D'_\perp(\delta'+1)\left(\frac{D'_\perp}{\delta'} - \frac{D_\perp^{s\prime}}{\eta'}\right) = 2. \tag{40}$$

Note that $D_\perp^{s\prime}$ and η' are known in terms of the input parameters via equations (28)–(30) [recalling that $D_\perp^{\rm 2D} = (I/2)^{1/2}$]. In particular,

$$D_\perp^{s\prime} = \frac{\sqrt{2 l_x l_y}}{\tilde{\lambda}}\frac{\eta}{\eta^2+1}\frac{f_s}{\sqrt{1-f_s}}\frac{b}{B_0} \tag{41}$$

$$\eta' D_\perp^{s\prime} = \frac{\sqrt{2} l_x}{\tilde{\lambda}}\frac{\eta^2}{\eta^2+1}\frac{1}{\xi}\frac{f_s}{\sqrt{1-f_s}}\frac{b}{B_0} \tag{42}$$

$$\frac{D_\perp^{s\prime}}{\eta'} = \frac{\sqrt{2} l_y}{\tilde{\lambda}}\frac{\xi}{\eta^2+1}\frac{f_s}{\sqrt{1-f_s}}\frac{b}{B_0}. \tag{43}$$

Now suppose that $\eta \to \infty$, while ξ is fixed. Then the terms $D_\perp^{s\prime}/\eta'$ and $\eta' D_\perp^{s\prime}$ go to zero and a constant, respectively. The coupled equations become

$$D'_\perp\left(\frac{1}{\delta'}+1\right)\left(\delta' D'_\perp - \eta' D_\perp^{s\prime}\right) = 2 \tag{44}$$

$$D'_\perp(\delta'+1)\left(\frac{D'_\perp}{\delta'}\right) = 2. \tag{45}$$

For this case, if $\eta' D_\perp^{s\prime} \ll 1$, which implies $D_x^{\rm slab} \ll D_x^{\rm 2D}$, the equations above are

$$D'_\perp\left(\frac{1}{\delta'}+1\right)\left(\delta' D'_\perp\right) = 2$$

$$D'_\perp(\delta'+1)\left(\frac{D'_\perp}{\delta'}\right) = 2.$$

The solutions are $D'_\perp \approx 1$ and $\delta' \approx 1$. That is, when $\eta \to \infty$ and $D_x^{\rm slab} \ll D_x^{\rm 2D}$, the diffusion coefficients tend to two-dimensional values ($D_i \approx D_i^{\rm 2D}$). If instead $\eta' D_\perp^{s\prime} \gg 1$, which implies $D_x^{\rm slab} \gg D_x^{\rm 2D}$, then considering equation (44) we know that $\delta' D'_\perp$ must be greater than $\eta' D_\perp^{s\prime}$ because the left-hand side of that equation needs to be positive. Thus, $\delta' > \eta' D_\perp^{s\prime}/D'_\perp$. From equation (45), we can write

$$\delta' = \frac{D_\perp'^2}{2 - D_\perp'^2} \tag{46}$$

and also

$$D'_\perp = \sqrt{\frac{2}{1+1/\delta'}}. \tag{47}$$

Here we note from equation (47) that $0 < D'_\perp < \sqrt{2}$, so $\delta' \gg 1$. This in turn implies $D'_\perp \approx \sqrt{2}$, and then equation (44) implies that $\delta' D'_\perp \approx \eta' D_\perp^{s\prime}$ and $\delta' \approx \eta' D_\perp^{s\prime}/\sqrt{2}$. Converting these to diffusion coefficients, the solutions for the case where $\eta \to \infty$ and $D_x^{\rm slab} \gg D_x^{\rm 2D}$ are $D_x \approx D_x^{\rm slab}$ and $D_y \approx 2D_x^{\rm 2D} D_y^{\rm 2D}/D_x^{\rm slab}$, which is much lower than $D_y^{\rm 2D}$. Paradoxically, the increased slab turbulence in the x-direction leads to *decreased* y-diffusion. That means that when $D_x^{\rm slab}$ makes D_x very large, it decorrelates the random flights in the y-direction and also decreases the mean free path in the y-direction and D_y. An analogous result in the case of field-line separation was found by Ruffolo et al. (2004).

If η instead goes to zero, the roles of x- and y-components are reversed. That is, if $D_y^{\rm slab} \ll D_y^{\rm 2D}$, then the diffusion coefficients tend to two-dimensional values. If, on the other hand, $D_y^{\rm slab} \gg D_y^{\rm 2D}$, then $D_y \approx D_y^{\rm slab}$ and $D_x \approx 2D_x^{\rm 2D} D_y^{\rm 2D}/D_y^{\rm slab}$, which is much lower than $D_x^{\rm 2D}$.

Finally, we consider the case where $\xi \to \infty$ for fixed η. It can be shown that if $D_\perp^{\rm slab} \gg D_\perp^{\rm 2D}$, then $D_i \approx D_i^{\rm slab}$. If $D_\perp^{\rm slab} \ll D_\perp^{\rm 2D}$, then $D_y \approx D_y^{\rm slab}$ while $D_x \approx 2D_x^{\rm 2D} D_y^{\rm 2D}/D_y^{\rm slab}$, which is again much lower than $D_x^{\rm 2D}$.

4. NUMERICAL CONFIRMATION

To confirm the conclusions of these analytic calculations, we have also performed computer simulations of the field-line random walk in nonaxisymmetric two-component turbulence. While the simulations inevitably involve some discretization and statistical errors, they do avoid the key assumptions of the analytic work (Corrsin's hypothesis and Gaussian probability distributions) and thus provide an independent check of their validity. For axisymmetric turbulence, these assumptions have been computationally verified for the field-line random walk (Gray et al. 1996) and for field-line separation (Ruffolo et al. 2004) to within ~15%.

In order to simulate nonaxisymmetric turbulence, we construct the power spectra differently in the x- and y-directions. For slab turbulence, we set the power spectrum for simulations as

$$P_{ii}^{\rm slab}(k_z) = \frac{C_i^{\rm slab}}{\left[1+(k_z\lambda_i)^2\right]^{5/6}}, \quad (i = x, y), \tag{48}$$

where $C_i^{\rm slab}$ is a normalization constant of the i-component, set so as to obtain the desired slab turbulence energy, and λ_i is the parallel correlation scale of the i-component, which is directly related to the correlation length l_i. For the two-dimensional component, we instead specify the power spectrum $A(k_x, k_y)$ because as discussed in § 2, the power spectra $P_{xx}^{\rm 2D}$ and $P_{yy}^{\rm 2D}$ can be written as

$$P_{xx}^{\rm 2D}(k_x, k_y) = k_y^2 A\left(k'_\perp\right)$$

$$P_{yy}^{\rm 2D}(k_x, k_y) = k_x^2 A\left(k'_\perp\right), \tag{49}$$

where $k'_\perp$ is defined in § 2. The function of A that we use for simulations is

$$A\left(k'_\perp\right) = \frac{C^{\rm 2D}}{\left[1+(k'_\perp l_\perp)^2\right]^{7/3}}. \tag{50}$$

This form of the two-dimensional spectrum also permits the axisymmetric case when $\xi = 1$. These forms of the slab and two-dimensional power spectra are consistent with a Kolmogorov power law in the omnidirectional power spectrum at high wavenumber (Ruffolo et al. 2004) while rolling over to constant values of $P_{ii}^{\rm slab}$ and A at small wavenumbers. They provide a reasonable description of observed power spectra in interplanetary space over the energy-containing and inertial ranges of turbulence (Jokipii & Coleman 1968; Bieber et al. 1996).

Now we have the spectra of magnetic turbulence. The relations between the magnetic field fluctuations and power spectra are

$$b_x^{\rm slab}(k_z) = \sqrt{P_{xx}^{\rm slab}}\, e^{i\phi_x(k_z)} \tag{51}$$

$$b_y^{\rm slab}(k_z) = \sqrt{P_{yy}^{\rm slab}}\, e^{i\phi_y(k_z)} \tag{52}$$

$$b_x^{\rm 2D}(k_x, k_y) = -ik_y\sqrt{A(k_x, k_y)}\, e^{i\phi(k_x, k_y)} \tag{53}$$

$$b_y^{\rm 2D}(k_x, k_y) = ik_x\sqrt{A(k_x, k_y)}\, e^{i\phi(k_x, k_y)}, \tag{54}$$

where ϕ is an independent random phase for each Fourier mode. After we generate the magnetic fluctuations in $\boldsymbol{k}$ space, we use inverse Fourier transforms to convert them to real space. Now we have a representation of two-dimensional and slab fluctuations in the simulation box. Next, the field-line equations

$$\frac{dx}{dz} = \frac{b_x(x,y,z)}{B_0}, \qquad \frac{dy}{dz} = \frac{b_y(x,y,z)}{B_0}, \tag{55}$$

are solved by a fourth-order Runge-Kutta method with adaptive step size control (Press et al. 1992).

After we get the positions of each field line, yielding the diffusion coefficients, values of $\langle \Delta x^2 \rangle$ and $\langle \Delta y^2 \rangle$ are averaged over

TABLE 1

DISCRETE THEORY AND SIMULATION RESULTS FOR THE DIFFUSION COEFFICIENTS AND THEIR DIFFERENCES WHEN WE VARY f_x, l_x, AND l_y FOR SLAB TURBULENCE ONLY

Run	f_x	l_x	l_y	D_x Theory	D_y Theory	D_x Simulation	D_y Simulation	ΔD_x (%)	ΔD_y (%)
1	0.50	1.0	1.0	0.09762	0.09762	0.09591	0.09632	−1.75	−1.33
2	0.25	1.0	1.0	0.04881	0.14644	0.04879	0.14400	−0.04	−1.67
3	0.75	1.0	1.0	0.14644	0.04881	0.14859	0.04815	+1.47	−1.35
4	0.50	1.0	2.0	0.09762	0.19200	0.09717	0.19738	−0.46	+2.80
5	0.50	1.0	0.5	0.09762	0.05016	0.09989	0.04875	+2.33	−2.81
6	0.50	2.0	1.0	0.19200	0.09762	0.19011	0.09640	−0.98	−1.25
7	0.50	0.5	1.0	0.05016	0.09762	0.04941	0.09661	−1.50	−1.03
8	0.75	1.0	2.0	0.14644	0.09600	0.14338	0.09625	−2.09	+0.26

the set of field lines at Δz much greater than the correlation length. Then we determine $D_x = \langle \Delta x^2 \rangle / (2\Delta z)$ and $D_y = \langle \Delta y^2 \rangle / (2\Delta z)$. To ensure that our set of field lines properly samples the ensemble of magnetic fluctuations and to avoid periodicity effects, we randomly set starting points of the field lines in the simulation box, change the realization of the two-dimensional component for every simulation, and trace the field lines to only a few percent of the box length L_z.

To verify the theory, we perform the simulations for three cases. For the first case, we confirm the theory for nonaxisymmetric slab turbulence with no two-dimensional component. The results from simulations are compared with the discrete theory, i.e., the solution to equations (27)–(30), in which the integrals used to determine l_x, l_y, $\langle b^2 \rangle^{\rm slab}$, and $\tilde{\lambda}$ are replaced by discrete sums over the actual Fourier modes used in the simulations. This helps reduce the effect of discrete Fourier modes on the comparison and allows us to better check the assumptions underlying the theory. We set $L_x = L_y = L_z = 100{,}000\lambda_x$ and trace the field lines over only 2.5% of L_z. The number of grid points is $N_z = 2^{22} \approx 4$ million. The parameters governing anisotropy for this case are f_{sx}/f_{sy}, λ_x, and λ_y. In the axisymmetric case, we usually set $\lambda_x = \lambda_y = 1$ and $f_{sx} = f_{sy} = 0.5$, where $f_{sx} = \langle b_x^2 \rangle^{\rm slab} / \langle b^2 \rangle$ and $f_{sy} = \langle b_y^2 \rangle^{\rm slab} / \langle b^2 \rangle$. If we change these three parameters to other values, the system becomes nonaxisymmetric. In this simulation we set $b/B_0 = 0.5$ as a constant for all runs. The simulation results are shown in Table 1, and they match the discrete theory quite closely.

In the second case, we simulate field lines in two-component models that are nonaxisymmetric only in the two-dimensional component but axisymmetric in the slab component ($D_x^{\rm slab} = D_y^{\rm slab}$). We maintain $f_{sx} = f_{sy} = 0.5 f_s$ and $\lambda_x = \lambda_y = 1$, and vary only the ellipticity ξ of $A(k_x, k_y)$. Therefore, we should have a constant $D_x^{\rm slab} = D_y^{\rm slab}$ for all of these runs. Moreover, we set $l_\perp = 1$ and $b/B_0 = 0.5$ and perform two sets of simulations, for $E^{\rm slab} : E^{\rm 2D} = 20 : 80$, a good approximation for the solar wind (Bieber et al. 1994, 1996), and for $E^{\rm slab} : E^{\rm 2D} = 80 : 20$. In the simulations, we trace 1000 field lines in the large box with $L_z = 100{,}000\lambda_x$ and $L_x = L_y = 200\lambda_x$. The numbers of grid points are $N_x = N_y = 4096$ and $N_z = 2^{22}$. Tables 2 and 3 indicate the numerical and theoretical values and their differences when we vary the ellipticity ξ for $E^{\rm slab} : E^{\rm 2D} = 20 : 80$ and $80 : 20$. The theoretical values and numerical results for those two cases are also plotted in Figures 3 and 4, respectively. For $E^{\rm slab} : E^{\rm 2D} = 20 : 80$, we add two columns in Table 2, with kurtosis values of each component, $\kappa_x \equiv \langle \Delta x^4 \rangle / \langle \Delta x^2 \rangle^2$ and $\kappa_y \equiv \langle \Delta y^4 \rangle / \langle \Delta y^2 \rangle^2$, to test for similarity to Gaussian distributions, which have a kurtosis of 3. We conclude that all kurtosis values are consistent with those of Gaussian distributions.

Finally, to be sure that the theory also works for various cases in which both the slab and two-dimensional turbulence are nonaxisymmetric, we independently vary the parameters that cause nonaxisymmetry of the two-component turbulent field. We use the box size and other parameters as previously, but vary f_{sx}/f_s, λ_x, λ_y, and ξ. Table 4 shows the results, which indicate reasonable agreement between simulations and the discrete theory.

5. SUMMARY

We analytically derive the field-line diffusion coefficients in the directions x and y, perpendicular to the mean field direction z, for nonaxisymmetric, two-component (2D+slab) turbulence, with variances transverse to the mean magnetic field. We are motivated to explore the nonaxisymmetric field-line random walk because of the measured nonaxisymmetry of magnetic fluctuations in the solar wind in the inner heliosphere, and the possibility that in the outer heliosphere there are substantial differences in the energies and correlation scales of fluctuations in the two perpendicular directions. The latter could be expected due to the much stronger divergence of the solar wind flow in the θ-direction compared with the r-direction, as well as the shorter distance scale

TABLE 2

COMPARISON BETWEEN NUMERICAL AND THEORETICAL RESULTS OF THE DIFFUSION COEFFICIENTS FOR 20% SLAB AND 80% TWO-DIMENSIONAL ENERGIES WHEN ξ IS VARIED

Run	ξ	D_x Theory	D_y Theory	D_x Simulation	D_y Simulation	ΔD_x (%)	ΔD_y (%)	$\kappa^x = \langle \Delta x^4 \rangle / \langle \Delta x^2 \rangle^2$	$\kappa^y = \langle \Delta y^4 \rangle / \langle \Delta y^2 \rangle^2$
1	0.25	0.0550	0.4038	0.0556	0.3767	+1.15	−6.72	2.90	3.05
2	1/3	0.0711	0.3748	0.0722	0.3449	+1.60	−7.98	3.00	3.01
3	0.5	0.1053	0.3172	0.1016	0.2771	−3.50	−12.64	3.01	2.95
4	2/3	0.1392	0.2692	0.1340	0.2386	−3.77	−11.36	3.15	3.05
5	1.0	0.2000	0.2000	0.1812	0.1778	−9.43	−11.10	3.09	2.97
6	1.5	0.2692	0.1392	0.2350	0.1310	−12.70	−5.88	3.04	3.01
7	2.0	0.3172	0.1053	0.2897	0.1021	−8.68	−3.02	2.98	2.93
8	3.0	0.3748	0.0711	0.3535	0.0699	−5.68	−1.73	3.02	2.95
9	4.0	0.4038	0.0550	0.3758	0.0572	−6.94	+4.07	3.02	2.89

TABLE 3

Comparison between Numerical and Theoretical Results of the Diffusion Coefficients for 80% Slab and 20% Two-dimensional Energies When ξ Is Varied

Run	ξ	D_x Theory	D_y Theory	D_x Simulation	D_y Simulation	ΔD_x (%)	ΔD_y (%)
1	0.25	0.0923	0.1508	0.0894	0.1651	−3.20	+9.44
2	1/3	0.0991	0.1574	0.0984	0.1653	−0.69	+5.06
3	0.5	0.1122	0.1595	0.1155	0.1688	+2.91	+5.84
4	2/3	0.1241	0.1554	0.1283	0.1636	+3.38	+5.27
5	1.0	0.1418	0.1418	0.1439	0.1448	+1.51	+2.16
6	1.5	0.1554	0.1241	0.1640	0.1275	+5.58	+2.72
7	2.0	0.1597	0.1123	0.1653	0.1119	+3.49	−0.41
8	3.0	0.1574	0.0991	0.1700	0.0981	+8.02	−0.93
9	4.0	0.1508	0.0923	0.1622	0.0904	+7.51	−2.09

between intermittent structures in the r-direction. We explore the nonaxisymmetric field-line random walk by adopting the additional assumptions of spatial homogeneity, the diffusion approximation, and Corrsin's independence hypothesis. The validity of the diffusion approximation and Corrsin's hypothesis is verified by numerical simulations that do not rely on these assumptions. The analytic results are nonperturbative in the sense that neither the turbulent energy of the slab nor the two-dimensional component is constrained to be small. The results also allow general and independent functional forms for the slab and two-dimensional power spectra.

We can see that the numerical results and theory are in quite good agreement. For pure nonaxisymmetric slab turbulence, the simulations agree very well with the theory, with differences less than 3% (Table 1). It is interesting to note the discrepancy between simulations and theory when $E_{\rm slab} : E_{\rm 2D} = 20 : 80$ (the energy ratio in the solar wind) and the field is nonaxisymmetric only in the two-dimensional component (see Fig. 3 and Table 2). This is large (9%–13%) when ξ is near 1, and it drops when $\xi \gg 1$ and $\xi \ll 1$. Moreover, the discrepancy in the direction that gives a large diffusion coefficient is always greater than that in the direction that gives a small value. When we decrease the fraction of turbulent energy in the two-dimensional component to 20% ($E_{\rm slab} : E_{\rm 2D} = 80 : 20$; see Fig. 4 and Table 3), the differences between theory and numerical results decrease. It seems that the two-dimensional turbulent energy affects the discrepancy between theory and simulations. However, the differences are still within 15%, which is similar to that obtained by Gray et al. (1996). Furthermore, the theory is also verified in the case where both slab and two-dimensional turbulence are nonaxisymmetric (Table 4).

The two-component model considered here is a particular case of anisotropic turbulence, in which power in $\boldsymbol{k}$ space is concentrated along the parallel (k_z) axis and along the perpendicular (k_x, k_y) plane, which has been shown to provide a useful description of solar wind turbulence and associated particle transport phenomena (Matthaeus et al. 1990; Bieber et al. 1994, 1996). For slab turbulence, we allow nonaxisymmetry in the form of independent power spectra in the x- and y-directions, i.e., a general polarization. For two-dimensional turbulence, one can have nonaxisymmetry in terms of stretching in one direction, so we consider a power spectrum $A(k_x, k_y)$ of the potential function that is constant along ellipses in (k_x, k_y). Some previous studies of nonaxisymmetric turbulence (e.g., Pommois et al. 1999, 2001) have instead considered an "ellipsoidal" power spectrum with no polarization and turbulent energy that is constant along ellipsoids in $\boldsymbol{k}$ space, which has the advantage of including oblique wavevectors, and the disadvantages that analytic calculations are more difficult and certain quantities cannot be varied independently, such as P_{ii} as $\boldsymbol{k} \rightarrow 0$ along different directions. The model differences are sufficiently great that we defer a proper comparison to future work.

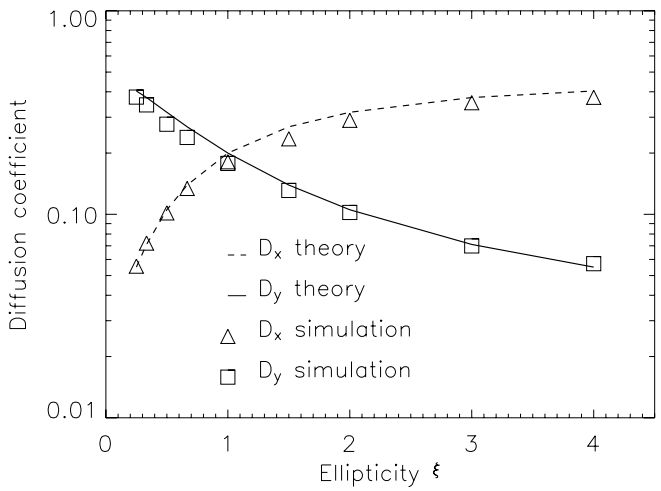

Fig. 3.—Diffusion coefficients from discrete theory and simulations for an energy ratio $E^{\rm slab} : E^{\rm 2D} = 20 : 80$, when we vary only the ellipticity ξ (see text for details).

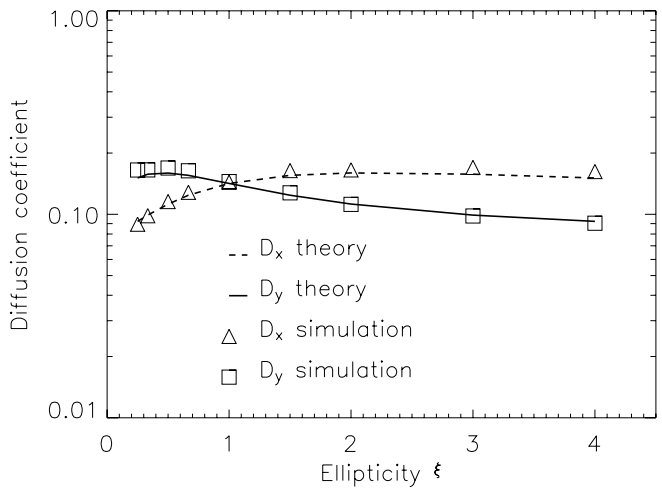

Fig. 4.—Diffusion coefficients from discrete theory and simulations for an energy ratio $E^{\rm slab} : E^{\rm 2D} = 80 : 20$, when we vary only the ellipticity ξ (see text for details).

TABLE 4

Comparison between Numerical and Theoretical Results of the Diffusion Coefficients When We Vary All Nonaxisymmetry Parameters

$E_{slab}:E_{2D}$	f_x	l_x	l_y	ξ	D_x Theory	D_y Theory	D_x Simulation	D_y Simulation	ΔD_x (%)	ΔD_y (%)
20:80	0.25	1.0	1.0	1.0	0.18260	0.21824	0.15744	0.20091	−13.78	−7.94
	0.5	1.0	2.0	1.0	0.18881	0.22193	0.17234	0.20854	−8.72	−6.03
	0.75	1.0	2.0	2.0	0.30971	0.11456	0.30420	0.10064	−1.78	−12.15
80:20	0.25	1.0	1.0	1.0	0.09353	0.19602	0.09823	0.19983	+5.02	+1.94
	0.5	1.0	2.0	1.0	0.14387	0.19154	0.13487	0.21980	−6.26	+14.75
	0.75	1.0	2.0	2.0	0.19869	0.10668	0.21412	0.10718	+7.77	+6.10

The solution for the diffusion coefficients in our model of nonaxisymmetric two-component turbulence is in the simple form of coupled biquadratic equations. We also show closed-form and limiting expressions for special cases of interest. In some cases there is a counterintuitive result that enhanced fluctuations in one direction lead to decreased diffusion in the other direction. This is because the long random flights in one direction tend to decorrelate the turbulence in the other direction. It is shown that extreme nonaxisymmetry always leads to diffusion coefficients proportional to the rms two-dimensional fluctuation (i.e., proportional to b/B_0). Since strong nonaxisymmetry might be expected in the outer heliosphere as the solar wind stretches differently in the two perpendicular (nonazimuthal) directions, this result is relevant to the heliospheric transport of charged particles, such as solar modulation of Galactic cosmic rays.

This research was partially supported by a Basic Research Grant and a Royal Golden Jubilee Fellowship from the Thailand Research Fund, the Rachadapisek Sompoj Fund of Chulalongkorn University, and the NASA Sun-Earth Connections Theory Program (grant NAG 5-8134).

REFERENCES

Belcher, J. W., & Davis, L., Jr. 1971, J. Geophys. Res., 76, 3534
Bieber, J. W., Matthaeus, W. H., Smith, C. W., Wanner, W., Kallenrode, M.-B., & Wibberenz, G. 1994, ApJ, 420, 294
Bieber, J. W., Wanner, W., & Matthaeus, W. H. 1996, J. Geophys. Res., 101, 2511
Burger, R. A., & Hattingh, M. 1998, ApJ, 505, 244
Chuychai, P., Ruffolo, D., Matthaeus, W. H., & Rowlands, G. 2005, ApJ, 633, L49
Corrsin, S. 1959, in Atmospheric Diffusion and Air Pollution, ed. F. Frenkel & P. Sheppard (New York: Academic Press), 161
Dasso, S., Milano, L. J., Matthaeus, W. H., & Smith, C. W. 2005, ApJ, 635, L181
Gray, P. C., Pontius, D. H., Jr., & Matthaeus, W. H. 1996, Geophys. Res. Lett., 23, 965
Isichenko, M. B. 1991a, Plasma Phys. Controlled Fusion, 33, 795
———. 1991b, Plasma Phys. Controlled Fusion, 33, 809
Jokipii, J. R. 1966, ApJ, 146, 480
———. 1973, ApJ, 182, 585
Jokipii, J. R., & Coleman, P. J. 1968, J. Geophys. Res., 73, 5495
Jokipii, J. R., Kóta, J., Giacalone, J., Horbury, T. S., & Smith, E. J. 1995, Geophys. Res. Lett., 22, 3385
Jokipii, J. R., & Parker, E. N. 1968, Phys. Rev. Lett., 21, 44
———. 1969, ApJ, 155, 777
Leamon, R. J., Smith, C. W., & Ness, N. F. 1998, Geophys. Res. Lett., 25, 2505
Matthaeus, W. H., Goldstein, M. L., & Roberts, D. A. 1990, J. Geophys. Res., 95, 20673
Matthaeus, W. H., Gray, P. C., Pontius, D. H., Jr., & Bieber, J. W. 1995, Phys. Rev. Lett., 75, 2136
Mazur, J. E., Mason, G. M., Dwyer, J. R., Giacalone, J., Jokipii, J. R., & Stone, E. C. 2000, ApJ, 532, L79
McComb, W. D. 1990, The Physics of Fluid Turbulence (Oxford: Clarendon Press)
Parker, E. N. 1958, ApJ, 128, 664
Pommois, P., Veltri, P., & Zimbardo, G. 1999, Phys. Rev. E, 59, 2244
———. 2001, Phys. Rev. E, 63, 066405
Press, W. H., Teukolsky, S. A., Vetterling, W. T., & Flannery, B. P. 1992, Numerical Recipes in FORTRAN (Cambridge: Cambridge Univ. Press)
Rechester, A. B., & Rosenbluth, M. M. 1978, Phys. Rev. Lett., 40, 38
Ruffolo, D., Matthaeus, W. H., & Chuychai, P. 2003, ApJ, 597, L169
———. 2004, ApJ, 614, 420
Salu, Y., & Montgomery, D. C. 1977, Phys. Fluids, 20, 1
Smith, C. W., Mullan, D. J., & Ness, N. F. 2004, J. Geophys. Res., 109, A01111
Smith, C. W., Mullan, D. J., Ness, N. F., Skoug, R. M., & Steinberg, J. 2001, J. Geophys. Res., 106, 18625
Taylor, J. B., & McNamara, B. 1971, Phys. Fluids, 14, 1492
Wang, H.-D., Vlad, M., Vanden Eijnden, E., Spineanu, F., Misguich, J. H., & Balescu, R. 1995, Phys. Rev. E, 51, 4844